Complete fusion and quasifission in reactions between heavy ions

B. B. Back
Chemistry Division, Argonne National Laboratory, Argonne, Illinois 60439
(Received 14 January 1985)

It is shown that fission anisotropies from reactions with projectiles lighter than $A=20$ are well described by the standard theory, in which it is assumed that the distribution of K values (projection of total spin I onto the symmetry axis) is determined at the fission saddle point. Angular anisotropies of symmetric fragments from heavy ion reactions with projectiles heavier than $A=24$ are, however, substantially larger than expected on the basis of this theory, an observation which recently led to the suggestion that the K values adjust adiabatically during the descent from saddle to scission such that the observed final K distributions reflect a thermal equilibrium at the scission point. The predictions of such scission point models are compared with the available experimental data and it is shown that they fail to reproduce the observed trends as a function of bombarding energy for most systems. It is concluded that the observed deviation from the saddle point theory can be explained as a dynamical inhibition of complete fusion with heavy projectiles. An analysis is carried out in which the fraction of the symmetric fragment cross section originating from the fission decay of completely fused compound nuclei can be estimated. The systematics of the inhibition to complete heavy ion fusion is discussed in the framework of the extra push model.

I. INTRODUCTION

Complete fusion between heavy ions can be thought of as a complete amalgamation of all the nucleons of the target and the projectile into a composite system formed inside the fission barrier. For systems leading to nonfissioning nuclei, this process is identified by either direct observation of the residue of the fused system after thermal evaporation of particles or by observation of characteristic gamma rays from the final steps of the decay process. There is little doubt that these observations are good signatures for complete fusion except, maybe, at higher beam velocities, where the emission of fast particles from the interacting ions prior to fusion may not be excluded experimentally.

In reaction systems leading to fissionable nuclei it has been possible to discriminate effectively against such incomplete fusion reaction by measuring the correlation angle between the two fragments from the subsequent fission decay of the fused system. This method ensures that the full momentum of the beam particle is transferred to the two final fission fragments, i.e., that there are no fast particles emitted in the forward direction prior to fusion as in the incomplete fusion reaction. Whether a completely fused system was formed during the process is not verified in such experiments, although this has often been an inherent assumption in the interpretation. That fission-like products with symmetric masses can result from reactions with the typical characteristics of a direct process, without proceeding through a step of complete fusion, has recently been demonstrated in reactions with ^{208}Pb and ^{238}U beams.[1,2] The observation of an increased width of the symmetric mass distribution in heavy ion reactions has also been interpreted as the consequence of an intermediate reaction mechanism.[3] It therefore appears that the observation of final fragments possessing the typical characteristics of the products from fission of a fused system may not be a good signature for complete fusion. In fact, it has been shown that the anisotropy of symmetric fragments from a variety of heavy ion reactions does not agree with the standard theory for fission angular distributions[4-10] although this model is very successful in accounting for the observed anisotropies in a large number of reactions with lighter ions.

It has been suggested that this deviation from the standard theory, which is observed only for projectiles heavier than $A=20$, is an indication of failure to produce a completely fused system in the reaction.[4-10] Recently it has also been suggested that large angular momenta and excitation energies encountered in heavy ion fusion reactions may tend to alter the distribution of K values during the descent from saddle to scission in such a way that the observed final K distribution may reflect a statistical distribution at the scission point.[11-13]

In the present work, these hypotheses are scrutinized by comparing the K distributions predicted by such scission point models and the standard saddle point model with experimentally determined values. It is found that the apparent success of the scission point models[11-13] hinges on unrealistic estimates of the appropriate phase space factors at the scission point. Using more realistic phase space factors results in large discrepancies between the predicted and measured K distributions in most cases. It is concluded that the change in the K distribution during the descent from saddle to scission is quite insignificant, even at the high temperatures and angular momenta experienced in ^{16}O and ^{19}F induced reactions, which are comparable to those of reactions with heavier projectiles. It therefore appears that the angular distribution of fission fragments from the decay of a rapidly rotating, highly excited compound system is determined at the saddle point. We therefore interpret the observed deviations from the saddle point model in the case of reactions induced by heavier projectiles as an indication that a large fraction of these reactions failed to produce completely fused systems inside the fission barrier and that the observed angular distributions reflect a significant contribution from more direct reactions in which an approximate equilibration of the mass asymmetry and energy degrees of freedom is achieved. This reaction channel is referred to as quasifission[14,15] or fast fission.[3,16]

In this paper we attempt to estimate the contribution of complete fusion to the observed cross section for symmetric fragmentation by analyzing the deviations of the observed fragment angular distributions from those predicted by the standard saddle point model. The results of this analysis are interpreted in the framework of the extra push model[15] and the systematics of the complete fusion inhibition in heavy ion reactions are investigated.

II. FISSION ANGULAR DISTRIBUTION THEORIES

The angular dependence of fission decays may in general be expressed in terms of the projection, K, of the total spin vector, I, onto the center axis of the separated fission fragments, normally denoted the fission axis, Fig. 1(c). If the fissioning system was formed by a full momentum transfer reaction between spin zero targets and projectiles, the total spin I has no component along the beam axis, i.e., $M=0$ and the angular distribution of fragments may be expressed as follows:

$$W(\theta)=\sum_{I=0}^{\infty}(2I+1)T_I\sum_{K=-I}^{I}\rho_I(K)\,|\,d^I_{0K}(\theta)\,|^2\,, \qquad (1)$$

where T_I is the combined probability for complete fusion and subsequent fission decay of the Ith partial wave and $\rho_I(K)$ is the normalized distribution of final K values.

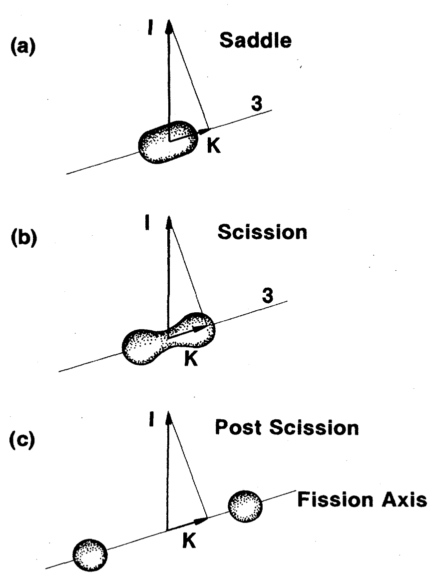

FIG. 1. Illustration of the various stages of the fission process, i.e., saddle, scission, and post scission.

$d(\theta)$ is the θ-dependent part of the symmetric top wave function (the $\mathscr{D}$ function). This expression is a general representation of angular distributions of two-body decays using the helicity representation.

The fusion-fission probability, T_I, is in the present work estimated in the following way. It is assumed that the fission probability is essentially unity for the very fissile systems considered in the present study. This assumption is supported by the experimental observation of very small evaporation residue cross sections in these systems. The spin dependence of the fusion probability is estimated in a simple model of the fusion of heavy ions which is based on the proximity description of the nuclear potential[9] and which includes the effects of static target deformations and zero point vibrations.[17] The parameters of the model are adjusted to reproduce the observed angle integrated fission cross sections which ensures that a reasonable description of the tail of the fusion cross sections at large angular momenta is achieved.

The main point of controversy is concerned with the estimate of the distribution of K values, $\rho_I(K)$. In the following we will discuss two different models for the estimate of this distribution, namely the saddle point model and the scission point model, which give quite different predictions for the width of the K distributions and, consequently, different fission anisotropies.

A. Saddle point model

In the standard theory, the distribution of K values is estimated by using a level density argument at the fission saddle point.[18] This approach leads to the expression

$$\rho(K)\propto\exp(-K^2/2K_0^2)\,, \qquad (2)$$

where

$$K_0^2=\frac{J_{\rm eff}}{\hbar^2}T_{\rm sad};\quad \frac{1}{J_{\rm eff}}=\frac{1}{J_{\parallel}}-\frac{1}{J_{\perp}}\,. \qquad (3)$$

The distribution of K values is therefore represented by a Gaussian with a standard deviation K_0, which is related to the nuclear temperature at the saddle point, $T_{\rm sad}$, and the moments of inertia, $J_{\parallel}$ and $J_{\perp}$, for rotations around axis parallel and perpendicular to the nuclear symmetry axis, respectively. These moments of inertia can be estimated by models describing the shape of the nucleus at the saddle point such as, e.g., the rotating liquid drop model.[19] The nuclear temperature at the saddle point, $T_{\rm sad}$, is given by

$$T_{\rm sad}=\left[\frac{E^*-B_f-E_{\rm rot}}{A/8.5}\right]^{1/2}, \qquad (4)$$

where E^* is the excitation energy of the fissioning system, B_f is the fission barrier, $E_{\rm rot}$ is the rotational energy of the system, and A is the mass number.

The basic assumption of the saddle point model is that the K value selected as the saddle point is traversed is unchanged during the descent from saddle to scission.[20] The validity of this assumption is not *a priori* well established, but it has been supported by a large number of both light and heavy ion induced fission studies over two decades.

Recently, it has also been supported by theoretical studies of the collective modes of dinuclear systems.[21] These studies show that the "tilting" mode, which is the only mode (out of six possible) which can change the internuclear orientation relative to the spin vector and therefore the K value, is only very weakly excited in nuclear collisions. Although the situation is somewhat different in the process of fission, this study does lend credibility to the assumption of K conservation during the descent from saddle to scission as assumed in the saddle point model.

B. Scission point models

In the scission point model[11–13] it is assumed that the K distribution is readjusted adiabatically during the descent from saddle to scission such that the fission anisotropy reflects a statistical distribution of K values at the scission point. Assuming that the system at scission rotates like a rigid body, one again finds that the distribution of K values is a Gaussian with a variance

$$K_0^2=\frac{J_{\mathrm{eff}}}{\hbar^2}T_{\mathrm{scis}};\quad \frac{1}{J_{\mathrm{eff}}}=\frac{1}{J_{\parallel}}-\frac{1}{J_{\perp}}\,, \tag{5}$$

where the moments of inertia, $J_{\parallel}$ and $J_{\perp}$, and the temperature, T_{scis}, refer to the scission shape. Estimating the values of K_0 in the scission point model is therefore reduced to a problem of estimating the scission shape and the nuclear temperature at that shape.

From the systematics of measured total kinetic energies in fission, E_K, we obtain a limit for the compactness of the system at scission by assuming that the observed kinetic energy arises solely from the Coulomb repulsion between the fragments at scission. This represents an upper limit for the Coulomb repulsion consistent with a completely damped motion from saddle to scission, which leaves no room for kinetic energy of the fragments when they arrive at scission. It should be kept in mind that the assumption of some prescission kinetic energy would result in a lower estimate of both the effective moment of inertia, J_{eff}, and the temperature, T_{scis}, leading to a decrease in the estimate of the value of K_0. The systematics of total kinetic energies in fission[22] is accurately reproduced by assuming that it represents the Coulomb repulsion between two coaxial spheroids of equal volume, separated by a distance of $d=2$ fm and with a ratio of minor to major axis of $a/c=0.58$. This shape uniquely determines the moments of inertia to be used in Eq. (5).

The temperature at scission is estimated from the relation

$$T_{\mathrm{scis}}=\left[\frac{E_{\mathrm{c.m.}}+Q_{\mathrm{sym}}-E_K-E_{\mathrm{def}}-E_{\mathrm{rot}}}{A/8.5}\right]^{1/2}, \tag{6}$$

where Q_{sym} is the reaction Q value for going to a symmetric mass split, E_{def} is the energy bound in fragment deformation estimated at 12 MeV from studies of low energy fission in the actinide region, $E_{\mathrm{c.m.}}$ is the center of mass energy of the reaction, E_{rot} is the rotational energy of the complex, and E_K is the Viola estimate[22] of the total kinetic energy, which presently is identified with the Coulomb repulsion energy at scission.

Recently, Bond[11,12] has studied the scission point model using a slightly different estimate of the K_0 parameter. He estimates the phase space factors at scission by assuming that the two fragments can rotate independently, i.e., not as a rigid body, under the condition of valid angular momentum couplings of the final channel spins and the orbital angular momentum to the total spin of the system. He shows that this gives rise to a Gaussian distribution of channel spins

$$\rho(S)=(2S+1)\exp[-(S+\tfrac{1}{2})^2/2S_0^2];\quad S_0^2=\frac{T_{\mathrm{scis}}}{\hbar^2}J_{\parallel}\,, \tag{7}$$

where $J_{\parallel}$ is the moment of inertia parallel to the symmetry axis assuming that the scission point configuration is represented by two touching spheres and the temperature at the scission point, T_{scis}, is computed according to Eq. (6) omitting, however, the deformation energy of the fragments. As pointed out by Rossner *et al.*[13] the fission angular distribution obtained from this approach is well approximated by Eq. (1) if K_0^2 is replaced by S_0^2 in the distribution of K values. The main differences between this approach and the one sketched above is that the relevant moment of inertia is the axial moment of inertia for a system of touching spheres, whereas using a more reasonable scission point configuration consistent with observed total kinetic energies leads to approximately 30% smaller estimates of K_0^2.

In a very similar approach, Rossner *et al.*[13] have studied the prediction of a scission point model in which the distribution of final K values is estimated from the distribution of channel spin. These authors assume a scission point configuration, which is consistent with the observed total kinetic energies in fission. The channel spin distribution is, however, estimated on the basis of fragment moments of inertia *perpendicular* to the symmetry axis. Since the generation of axial spin components, K, depends on the moments of inertia around the symmetry axis, this approach appears unjustified and it leads to an overestimation of the K_0^2 parameter of a factor of 2 compared with the rigid scission point estimate of Eq. (5).

C. Comparison with data, evidence for complete fusion inhibition

Since the different models for angular distributions all give rise to Gaussian K distributions it is sufficient to compare the predicted K_0^2 values with those obtained from an analysis of experimental fission angular anisotropies.[9] The results of such a comparison with recent experimental data is shown in Fig. 2. We observe that the saddle point model (solid curves) gives an excellent account of the observed K_0^2 values for the $^{19}F+^{208}Pb$ and $^{16}O+^{232}Th$ reactions, whereas it slightly overpredicts the K_0^2 values for the $^{16}O+^{238}U$ reaction. In contrast, neither the dependence on excitation energy nor the absolute values of K_0^2 are reproduced by the rigid scission point model (dashed curves). The scission point models by Bond[11,12] (dot-dashed curves) and Rossner *et al.*[13] (dotted curves) approximate the measured values of K_0^2 at the lower excitation energies, but fail to reproduce the observed increase with excitation energy, which reflects the

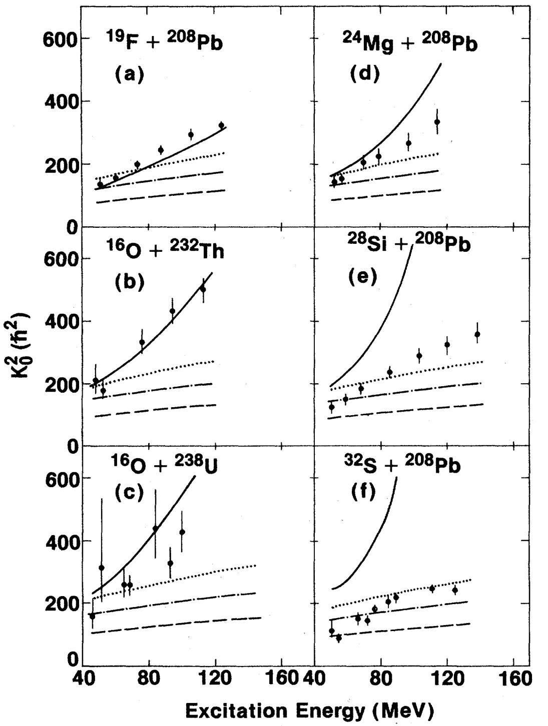

FIG. 2. Comparison of K_0^2 values derived from the analysis of experimental fission anisotropies with the prediction of the saddle point model (solid curves) and the rigid coaxial spheroids scission point model (dashed curves) as a function of excitation energy of the fissioning systems. The prediction of the scission point models of Refs. 12 and 13 are represented by the dot-dashed and dotted curves, respectively.

contraction of the scission point with angular momentum as predicted by the rotating liquid drop model.[19] The experimental K_0^2 values for the system ^{24}Mg + ^{208}Pb are compared to the model predictions in Fig. 2(d). For this system we observe a deviation of the experimental points from the predictions of the saddle point model although they still are very far from the rigid scission point model predictions. This trend is enhanced for the ^{28}Si + ^{208}Pb and the ^{32}S + ^{208}Pb reactions although the limit of K equilibration at the scission point, represented by the predictions of the rigid scission point model, is not reached even in these reactions. The scission point models of Bond[11,12] and Rossner *et al.*[13] are able to account for some of the data points of these reactions, although they fail to account for the dependence on the excitation energy.

In the reactions ^{16}O + ^{232}Th, ^{28}Si + ^{208}Pb and ^{16}O + ^{238}U, ^{32}S + ^{208}Pb, compound systems of equal fissility would be formed if both reactions led to complete fusion. Overlapping ranges of angular momentum and excitation energy are covered in both reactions. The observed differences in K_0^2 values therefore *cannot* be explained by a breakdown of the saddle point model at temperatures and angular momenta explored in these studies. Instead we are forced to conclude[5,9] that these differences arise from the breakdown of the assumption of complete fusion for the heavy projectiles. A substantial fraction of the cross section for symmetric mass products *must* originate from reactions which fail to produce a completely fused system inside the fission barrier. Otherwise, the reactions Si,S + Pb should have shown K_0^2 values similar to those of the O + Th,U reactions, respectively, as predicted by both saddle and scission point models.

Having reached the conclusion that only a fraction of the symmetric mass cross section in the reactions of Mg and heavier projectiles comes from the fission decay of completely fused systems, we will in Sec. III attempt to estimate the magnitude of this fraction of the cross section. This is done by assuming that it is associated with the lowest partial waves and that the subsequent fission decay occurs according to the saddle point model, guided by the success of this model to describe the fission anisotropies from reactions with lighter projectiles.

III. QUASIFISSION CONTRIBUTION

When attempting to divide the fission cross section into one part stemming from compound nucleus reactions and another part associated with quasifission, we shall first define a procedure for calculating "standard" angular distributions for the two types of reactions. From the systematics of $J_0/J_{\rm eff}$ values, obtained from a recent analysis of a large amount of fission angular distribution data,[9] we find that the $J_0/J_{\rm eff}$ values for compound nucleus fission is given by the rotating liquid drop model (RLDM),[19] using, however, a redefined value of the fissility parameter, namely

$$x' = x_{\rm RLDM} + 0.03 \ . \tag{8}$$

The standard RLDM fissility, $x_{\rm RLDM}$, is given by

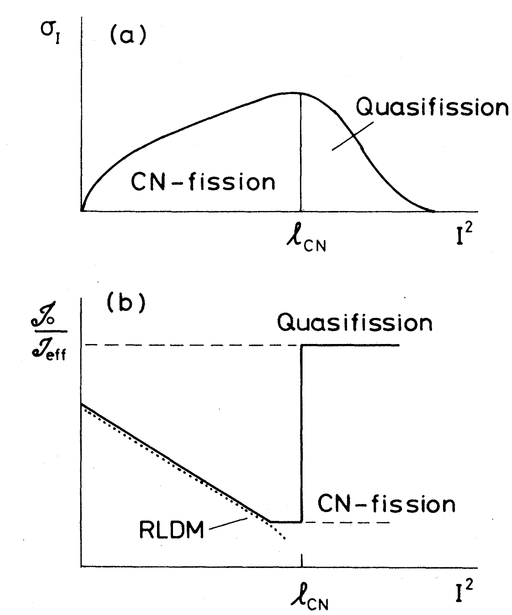

FIG. 3. Schematic illustration of the assumed division of the partial cross sections for complete fusion and quasifission reactions (a), and the associated values of $J_0/J_{\rm eff}$ (b).

$$x_{\rm RLDM}=\frac{Z^2/A}{50.883\{1-1.7826[(N-Z)/A]^2\}}\ . \tag{9}$$

With this redefinition, we obtain agreement with the α-induced data, as required, since these reactions are expected to proceed only through compound nucleus formation.

For compound nucleus fission we therefore use the following prescription for the $J_0/J_{\rm eff}$ values,

$$\frac{J_0}{J_{\rm eff}}=\max(a+bI^2,0.3)\ , \tag{10}$$

where $a=J_0/J_{\rm eff}(x',I=0)$ and b is the associated theoretical rate of decrease of $J_0/J_{\rm eff}$ with the squared spin of the fissioning nucleus. A minimum value of $J_0/J_{\rm eff}=0.3$ is chosen in order to simulate possible K breaking for systems with nearly spherical saddle points, low barriers, and large angular momenta, Fig. 3.

Somewhat arbitrarily we associate quasifission reactions with a value of $J_0/J_{\rm eff}=1.5$ independent of angular momentum. This exceeds the largest value obtained from the analysis of the experimental data.[9] In this analysis, we furthermore assume that the compound nucleus (CN) cross section corresponds to l values from zero up to a value of $l_{\rm CN}$(to be determined in the analysis), above which the reaction proceeds via quasifission, i.e.,

$$\frac{J_0}{J_{\rm eff}(l)}=\max(a+bl^2,0.3);\quad l<l_{\rm CN}\ ,$$

$$=1.5;\quad l>l_{\rm CN}\ . \tag{11}$$

This corresponds qualitatively to the dependence of K_0^2 on angular momentum proposed by Vandenbosch.[23]

The values of $l_{\rm CN}$ and the corresponding cross sections for complete fusion and quasifission are listed in Table I for the reactions analyzed using this procedure. The deduced compound nucleus cross sections are shown as solid triangles in Fig. 4. Since the determination of the complete fusion cross sections from fragment angular distributions, as outlined above, is based on a somewhat arbitrary assumption about the anisotropy associated with quasifission reactions, it is necessary to investigate the sensitivity of the resulting complete fusion cross sections to this assumption. In Fig. 5 we show the effect of assuming that the K distributions for quasifission are associated with shapes of the intermediate complex represented by touching spheres (open circles) and the scission point shape (solid dots). These two shapes correspond to

TABLE I. Experimental complete fusion cross sections deduced from fragment angular distribution.

Reaction	$E_{\rm lab}$ (MeV)	$l_{\rm CN}$ ($\hbar$)	$\sigma_{\rm CN}$ (mb)	E_{xx} (MeV)
^{19}F + ^{208}Pb	110	38±4	545±90	3.0±2.0
	120	47±4	765±90	4.9±2.9
	135	61±4	1090±90	4.6±2.7
	150	71±3	1260±70	6.4±2.2
	170	79±2	1355±60	11.3±2.5
	190	84±2	1490±40	19.5±2.0
^{24}Mg + ^{208}Pb	140	34±6	255±80	4.9±2.3
	145	39±4	360±65	5.6±2.0
	160	56±4	630±70	7.4±2.5
	170	61±4	725±80	11.5±3.0
	190	73±3	930±80	17.5±3.2
	210	83±4	1140±100	21.0±5.2
^{28}Si + ^{208}Pb	160	24±10	110±60	6.8±2.2
	170	35±6	220±65	10.8±2.5
	180	48±4	385±65	13.2±2.5
	200	63±4	555±70	20.0±3.3
	220	78±3	750±60	23.5±3.1
	240	88±4	920±80	28.4±4.8
	260	96±4	1070±90	33.5±5.5
^{32}S + ^{197}Au	185	30±10	105±60	9.0±2.8
	198	45±8	260±80	10.6±4.3
	219	65±4	550±60	15.2±3.0
	225	64±4	420±50	21.0±3.8
^{32}S + ^{208}Pb	198	36±6	185±55	12.7±3.1
	210	46±3	315±35	17.2±1.8
	219	53±3	375±40	20.1±2.5
	225	57±3	365±50	22.4±3.0
	250	69±2	535±30	32.0±2.2

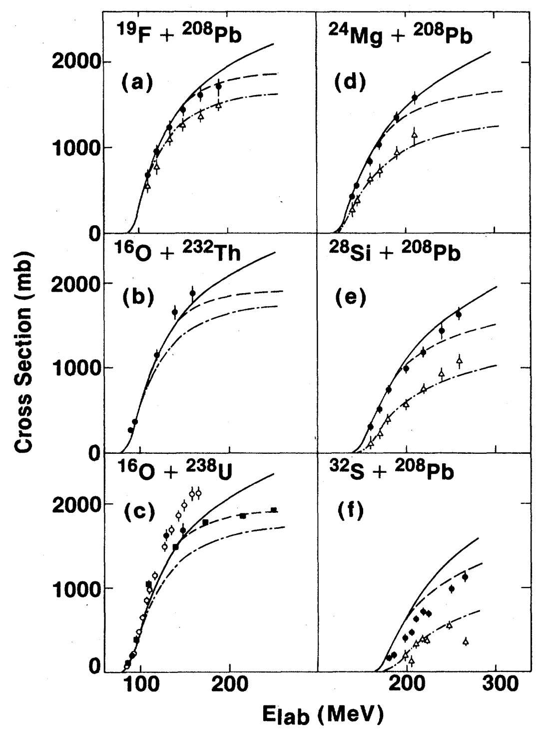

FIG. 4. Comparison of experimental cross sections with theoretical model calculations. Filled circles represent fission cross sections (Ref. 7), open circles are taken from Ref. 24 (^{16}O + ^{238}U), and solid squares represent measurements in which full momentum transfer was required (Refs. 10 and 25). The solid triangles represent the deduced complete fusion cross section. The calculated cross sections for touching (solid curves), capture (dashed curves), and complete fusion (dashed-dotted curves) are shown.

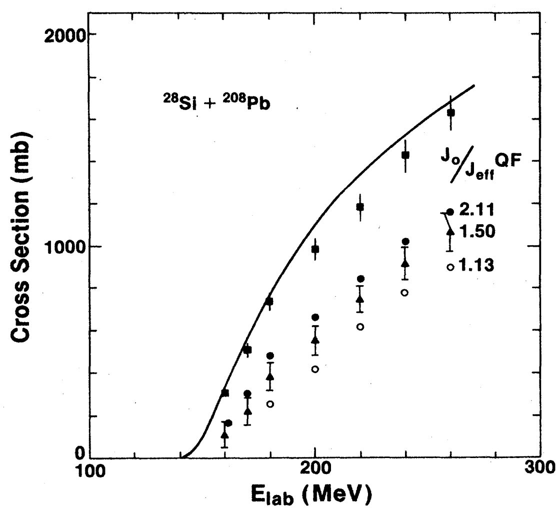

FIG. 5. Complete fusion cross sections determined under the assumption that the effective moment of inertia, $J_0/J_{\rm eff}$, takes values corresponding to touching spheres (1.13, open circles), the scission shape (2.11, solid dots), and an intermediate shape used in the present analysis (1.50, solid triangles). Measured total fission cross sections (solid squares) and calculated touching cross sections (solid curve) are included for comparison.

values of $J_0/J_{\rm eff}$ of 1.13 and 2.11, respectively. It is believed that this range of shapes will include the shapes at which the K distributions are determined in a quasifission reaction. It is observed that the deduced values of the complete fusion cross section are just barely outside the statistical error bars. The systematic error on the deduced complete fusion cross section, associated with the unknown anisotropy for quasifission reactions, is estimated to be less than about 30—40%.

IV. CROSS SECTIONS

A. Capture

The cross sections for capture, which encompasses quasifission and complete fusion reactions, is in the present work estimated on the basis of the extra push model.[14,15] The capture cross section is in this model associated with reactions which proceed inside the conditional (fixed entrance channel mass asymmetry) saddle point. For heavy projectiles, a radial injection energy which exceeds the interaction barrier by an amount E_x is needed. It is given by

$$E_{\rm c.m.}=E_x+V(l)\ , \tag{12}$$

where E_x is called the extra push energy and $V(l)$ is the angular momentum dependent interaction barrier.[2,9]

The extra push energy E_x follows a simple relationship,

$$E_x=E_{\rm ch}\cdot a^2(x'_{\rm Bass}-x'_{\rm th})^2\ , \tag{13}$$

where $E_{\rm ch}$ is the characteristic energy of the system,

$$E_{\rm ch}=\frac{2048}{81}\left[\frac{\pi}{3}\right]^{4/3}\frac{m\gamma r_0^6}{\hbar^2}\frac{A_1^{1/3}A_2^{1/3}(A_1^{1/3}+A_2^{1/3})^2}{A}\ , \tag{14}$$

and a and $x'_{\rm th}$ are parameters of the model, which have been determined from the analysis of experimental data. The radius parameter is $r_0=1.16$ fm, which is consistent with a surface tension coefficient of

$$\gamma=1.2496\{1-2.3[(N-Z)/A]^2\}\ .^9$$

The atomic mass unit is denoted m. The system parameter $x'_{\rm Bass}$ is given in terms of the balance of forces at the distance of maximum attraction, i.e.,

$$x'_{\rm Bass}=1.2\frac{F_{\rm Coul}+F_{\rm cent}}{(F_{\rm nucl})_{\rm max}}\ . \tag{15}$$

In the estimation of the centrifugal force, $F_{\rm cent}$, it is assumed that only a fraction, f, of the total angular momentum remains in the orbital motion. From the analysis of capture cross sections in ^{208}Pb and ^{238}U induced reactions, values of $x'_{\rm th}=0.70$, and $a=7(^{238}{\rm U})$ and $a=10(^{208}{\rm Pb})$ have been found. The angular momentum fraction f obtained in this analysis ranges from $f=0.54$—0.65.

We have estimated the capture cross sections for the reactions of the present study using the parameters, $a=7$, $x'_{\rm th}=0.70$, and $f=0.55$. Calculated capture cross sections are represented by dashed curves in Fig. 4. We observe that the part of the measured fission cross section which is associated with capture reactions (this excludes sequential fission) is reasonably well described by the calculations for ^{16}O and ^{19}F induced reactions. For the heavier projectiles (^{24}Mg and ^{28}Si) in reactions on ^{208}Pb targets, where the sequential fission contribution is strongly suppressed by the low fissility of targetlike reaction products, we see that the calculated capture cross section is slightly underestimated. This discrepancy could be removed by decreasing the value of the angular momentum fraction f for these systems. Such a change seems, however, unjustified and we conclude that the extra push model does not seem to be able to account for these cross sections.

B. Complete fusion

For heavy projectiles, the extra push model predicts that an extra-extra radial injection energy, over and above the extra push energy needed to induce capture, is required for the formation of a compound nucleus inside the true fission saddle point (fission barrier). Thus

$$E_{\rm c.m.}\geq E_{xx}+V(l)\ . \tag{16}$$

The extra-extra push energy, E_{xx}, can be estimated from the fusion cross sections $\sigma_{\rm CN}$, deduced from the analysis of the angular distributions. We approximate the l-dependent interaction barrier by

$$V(l)=V_0+\frac{\hbar^2 l^2}{2\mu R_0^2}\ , \tag{17}$$

where V_0 is the s-wave interaction barrier, μ is the reduced mass, and R_0 is the center distance for the s-wave barrier. The largest l wave contributing to the fusion and touching cross sections, respectively, are determined from the relations

$$E_{\text{c.m.}} = V_0 + \frac{l_{\text{touch}}^2 \hbar^2}{2\mu R_0^2} \quad (18)$$

and

$$E_{\text{c.m.}} = V_0 + E_{xx} + \frac{l_{\text{CN}}^2 \hbar^2}{2\mu R_0^2} . \quad (19)$$

The touching cross section, σ_{touch}, encompasses reactions which traverse the interaction barrier $V(l)$. Since, in the sharp cutoff model, the cross section is proportional to the square of the maximum l wave, we find

$$\frac{\sigma_{\text{CN}}}{\sigma_{\text{touch}}} = \frac{l_{\text{CN}}^2}{l_{\text{touch}}^2} = 1 - \frac{E_{xx}}{E_{\text{c.m.}} - V_0} \quad (20)$$

or

$$E_{xx} = (E_{\text{c.m.}} - V_0)\left[1 - \frac{\sigma_{\text{CN}}}{\sigma_{\text{touch}}}\right] . \quad (21)$$

The extra-extra push energies, E_{xx}, obtained from this relation are listed in Table I. The extra push model predicts the following relation,

$$E_{xx} = E_{\text{ch}} \cdot a''^2 [x_m(l) - x_{\text{th}}]^2 , \quad (22)$$

where x_{th} is the threshold parameter and $x_m(l)$ is the angular momentum dependent mean fissility tentatively given by[15]

$$x_m(l) = \sqrt{\infty x_m} + f\left[\frac{l}{l''_{\text{ch}}}\right]^2 . \quad (23)$$

where $x_m = \sqrt{x \cdot x'_{\text{Bass}}} - x(1 - \sqrt{x'_{\text{Bass}}/x})^2$. In this expression x is the fissility of the compound nucleus and l''_{ch} is a characteristic angular momentum given by

$$l''_{\text{ch}} = \sqrt{l'_{\text{ch}} l_{B_f=0}}/(1-x)^{1/4} , \quad (24)$$

where $l_{B_f=0}$ is the spin at which the fission barrier vanishes. l'_{ch} is the characteristic angular momentum for capture, i.e., the angular momentum at which the maximum nuclear force $(F_{\text{nucl}})_{\max}$ and the centrifugal force F_{cent} balance each other in the entrance channel.[2] In order to ascertain whether the experimentally determined extra-extra push energy depends on the system parameter $x_m(l)$ in the expected way we have plotted the quantity $(E_{xx}/E_{\text{ch}})^{1/2}$ as a function of $(l_{\text{CN}}/l''_{\text{ch}})^2$ for four reactions for which several bombarding energies were measured and the l dependence can be studied. The results are shown in Fig. 6. We find that the expected linear relationship between the two plotted parameters is indeed suggested by the data.

The expected increase of $(E_{xx}/E_{\text{ch}})^{1/2}$ with projectile mass is also found in the data. This is illustrated in Fig. 7, where the values of $(E_{xx}/E_{\text{ch}})^{1/2}$ determined from angular distribution data extrapolated to $l=0$ are plotted as a function of the mean fissility $x_m = x_m(l=0)$ for a number of reactions. From this analysis, which includes also data for ^{197}Au, ^{209}Bi, and ^{238}U targets, we find the linear relationship expected on the basis of Eqs. (22) and (23) using the parameters $a''=8\pm2$ and $x''_{\text{th}}=0.63\pm0.03$. The smooth dependence of $(E_{xx}/E_{\text{ch}})^{1/2}$ shows no indication of the "cliff," which was predicted theoretically from the

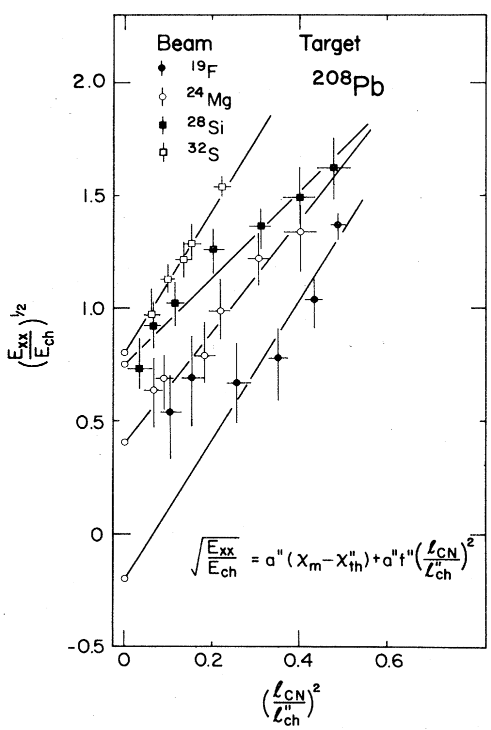

FIG. 6. Experimental values of the square root of the extra-extra push energy are shown as a function of the squared maximum angular momentum leading to complete fusion for reactions of ^{19}F, ^{24}Mg, ^{28}Si, and ^{32}S + ^{208}Pb.

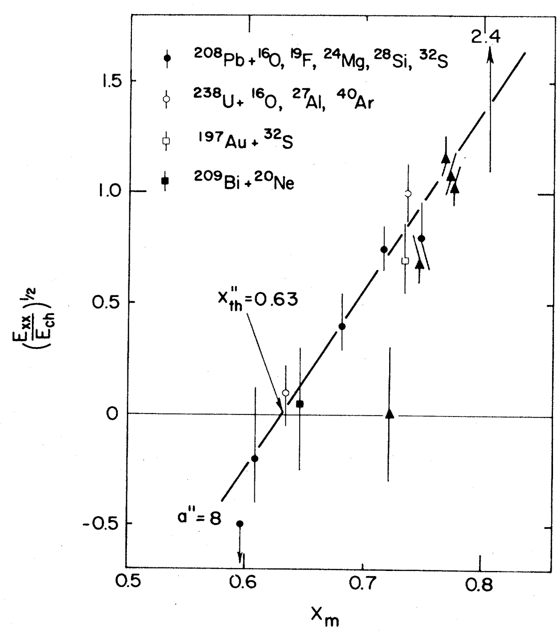

FIG. 7. The square root of the extrapolated extra-extra push energy for central ($l=0$) collisions is shown as a function of the mean fissility, x_m.

initial highly schematical model. This would have resulted in an abrupt increase in the deduced value of (E_{xx}/E_{ch}) when the x_m parameter reached the value x_{cliff}. Previous estimates of the value of x_{cliff} range from $x_{cliff}=0.85$ to 0.76. The present study indicates that $x_{cliff}<0.68$ since the presence of an extra-extra push is observed only for reactions of ^{24}Mg (+ ^{208}Pb) and heavier projectiles.

The angular momentum dependence of the extra-extra push energy is consistent with an angular momentum fraction of $f=0.4$. The fact that the f value determined from the complete fusion cross sections is substantially lower than those extracted from the capture cross sections (0.54—0.65) probably indicates that the tentatively proposed form of the mean fissility is inadequate.[15] Along with the experimentally determined values of $a''=8\pm2$ and $x''_{th}=0.63\pm0.03$, this value is used to calculate the complete fusion cross sections, which are represented by dot-dashed curves in Fig. 4. As expected, there is good agreement with the experimental complete fusion cross sections deduced from the fragment angular distributions.

For comparison, we also include recent experimental determinations of the extra-extra push energy from a study of complete fusion in symmetric or nearly symmetric systems by means of evaporation residue measurements.[26] These data are represented by solid triangles in Fig. 7. We observe that there is a surprisingly good agreement between the two sets of data, (obtained by entirely different methods), except for the ^{90}Zr + ^{90}Zr point, which falls outside the systematics. The reason for this deviation is not well understood, although it may be associated with the shell closure of these reaction partners.

Correlating the experimentally determined extra-extra push energies with the mean fissility x_m, as was done in the preparation of Fig. 7, relies on the validity of plausible, but untested, scaling laws of the extra-push model. In order to obtain a global view of the inhibition of complete fusion, we construct a map of the experimental extra-extra push energies as a function of the target (Z_2) and projectile (Z_1) charge numbers, see Fig. 8. We see that the measurements seem to follow smooth contours, shown for extra-extra push energies of $E_{xx}=0$, 10, and 20 MeV. The dashed curve represents the locus above which an extra push energy is required to induce capture, as observed in several studies. We observe that the $E_x=0$ and $E_{xx}=0$ contours merge for symmetric systems as expected, because the capture and complete fusion reactions, per definition, are inseparable for such systems. The dotted curve in Fig. 8 represents the locus at which the fission barrier vanishes. Since this curve lies above the contour, at which the extra-extra push sets in $(E_{xx}=0)$, it is apparent that the dynamical inhibition of the complete reaction is *always* more severe than the requirement of a finite fission barrier ensuring the stability of the compound system.

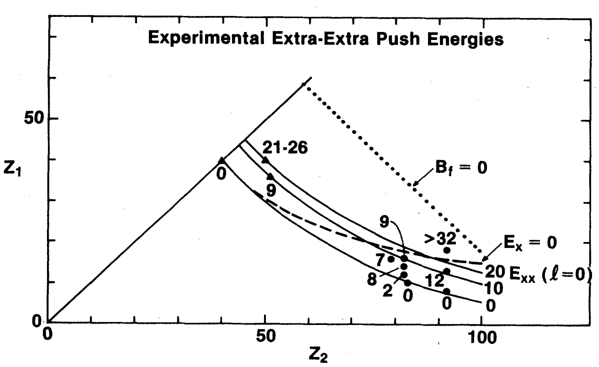

FIG. 8. Experimentally determined extra-extra push energies are displayed (MeV) in a Z_1 vs Z_2 map. Data points obtained from the analysis of fragment angular distributions are represented by solid circles, whereas solid triangles represent extra-extra push energies obtained from evaporation residue measurements (Ref. 26). Solid curves represent contours of equal extra-extra push energies drawn by hand on the basis of the data. The dashed curve represents the locus above which extra push energies are required to induce capture. This curve is drawn on the basis of parameters determined in Ref. 2.

The following picture emerges from the present analysis. Starting from reactions between "light" heavy ions (below the $E_{xx}=0$ curve in Fig. 8) complete fusion will occur if the interaction barrier is traversed. The total reaction cross section will therefore consist of just two components: quasielastic scattering (plus transfer) and complete fusion. Upon an increase of the projectile and/or target masses one *first* encounters the quasifission reaction and only after a *further* increase do the deep inelastic scattering reactions make their appearance. Thus the systematic ordering is the inverse of the historic sequence of observation.

Fusion cross sections calculated with the extra-extra push formalism using the presently deduced parameters are shown as dashed curves in Fig. 4. We see that the agreement with the experimental fusion cross sections extracted from the analysis is good as could be expected since the parameters are deduced from the very same cross sections. It would be interesting to test the predictive power of the extra-extra push model, with the presently adopted parameters, by comparing with measurements of evaporation residues, where one knows positively that fusion has taken place. For heavy systems, the extraction of an experimental fusion cross section from the measured evaporation residue cross section requires an accurate knowledge of the branching ratio for fission and neutron decay, which introduces large uncertainties also in these estimates of the fusion cross section and places such a comparison outside the scope of the present work.

V. SUMMARY

In the present work, is has been shown that the angular distributions of fragments from the fission decay of compound nuclei formed by complete fusion reactions with heavy ion projectiles are consistent with those expected on the basis of the saddle point model of fission. This model is based on the assumption that the K distribution is unchanged during the descent from saddle to scission. The fact that the saddle point model gives a good account of the angular distributions shows that this assumption is well justified, even in the case of high temperatures and angular momenta as encountered in such reactions. On the other hand, it appears that the recently proposed concept that the fission anisotropies should be determined by a statistical distribution of K states at the scission point is in contradiction with the data, both in terms of absolute value and dependence on excitation energy of the K_0^2 values. It is shown that the apparent success of these scission point models[11–13] is largely due to inconsistencies in the evaluations of the phase space factors at the scission point.

On the basis of a systematic comparison of fission anisotropies obtained in reactions with projectiles of varying mass, it is concluded that the deviations from the predictions of the saddle point model, which is observed for the heavier projectiles, $A > 20$, is caused by a failure to achieve complete fusion in these cases and not by a sudden change in the fission decay. Following this conclusion, it is attempted to determine the fraction of the cross section originating from complete fusion reactions. It is found that this fraction decreases with projectile mass and energy. The reduction in complete fusion cross section is expressed in terms of an extra-extra push energy, E_{xx}, which is required in excess of the interaction barrier in order to induce complete fusion in accordance with concepts of the extra push model.[14,15] The scaling of this extra-extra push energy is studied by including published data for complete fusion in nearly symmetric systems in the analysis.

The concept of an abrupt increase in E_{xx} (the cliff[14]) as a function of the means fissility, X_m, is not supported by the present analysis. The threshold, for the onset of the extra-extra push obtained from the present analysis, $x_{th} = 0.63 \pm 0.02$, is significantly lower than those obtained from the analysis of capture cross sections, $x_{th} = 0.70$.[1,2,14] This discrepancy may be due to a deficiency in the scaling properties of the extra push model.

ACKNOWLEDGMENTS

The author has profitted greatly from many stimulating and elucidating discussions with S. Bjørnholm. The hospitality of the faculty of the Niels Bohr Institute, Copenhagen, where part of the present work was carried out, is greatly appreciated. This work was supported in part by the Danish Natural Science Research Council. This work was performed under the auspices of the Office of High Energy and Nuclear Physics, Division of Nuclear Physics, U.S. Department of Energy, under Contract Number W-31-109-ENG-38.

[1]R. Bock, Y. T. Chu, M. Dakowski, A. Gobbi, E. Grosse, A. Olmi, H. Sann, D. Schwalm, U. Lynen, W. Müller, S. Bjørnholm, H. Esbensen, W. Wölfli, and E. Morenzoni, Nucl. Phys. **A388**, 388 (1982).

[2]J. Toke, G. X. Dai, S. Gralla, A. Gobbi, K. D. Hildenbrand, W. F. J. Müller, A. Olmi, H. Stelzer, B. B. Back, and S. Bjørnholm, Nucl. Phys. (to be published).

[3]C. Lebrun, F. Hanappe, J. F. Lecolley, F. Lefebvres, C. Ngô, J. Peter, and B. Tamain, Nucl. Phys. **A321**, 207 (1979).

[4]B. B. Back, H.-G. Clerc, R. R. Betts, B. G. Glagola, and B. D. Wilkins, Phys. Rev. Lett. **46**, 1068 (1981).

[5]B. B. Back, R. R. Betts, K. Cassidy, B. G. Glagola, J. E. Gindler, L. E. Glendenin, and B. D. Wilkins, Phys. Rev. Lett. **50**, 818 (1983).

[6]K. T. Lesko, S. Gil, A. Lazzarini, V. Metag, A. G. Seamster, and R. Vandenbosch, Phys. Rev. C **27**, 2999 (1983).

[7]M. B. Tsang, H. Utsunomiya, C. K. Gelbke, W. G. Lynch, B. B. Back, S. Saini, P. A. Baisden, and M. A. McMahan, Phys. Lett. **B129**, 18 (1983).

[8]M. B. Tsang, D. Ardouin, C. K. Gelbke, W. G. Lynch, Z. R. Xu, B. B. Back, R. R. Betts, S. Saini, P. A. Baisden, and M. A. McMahan, Phys. Rev. C **28**, 747 (1983).

[9]B. B. Back, R. R. Betts, J. E. Gindler, B. D. Wilkins, S. Saini, M. B. Tsang, C. K. Gelbke, W. Lynch, M. A. McMahan, and P. A. Baisden, Phys. Rev. C (to be published).

[10]J. Toke, R. Bock, Dai Guang-xi, A. Gobbi, S. Gralla, K. D. Hildenbrand, J. Kuzminski, W. F. J. Müller, A. Olmi, W. Reisdorf, S. Bjørnholm, and B. B. Back, Phys. Lett. **142B**, 258 (1984).

[11]P. Bond, Phys. Rev. Lett. **52**, 414 (1984).

[12]P. Bond (unpublished).

[13]H. H. Rossner, J. R. Huizenga, and W. U. Schröder, Phys. Rev. Lett. **53**, 38 (1984).

[14]W. J. Swiatecki, Phys. Scr. **24**, 113 (1981).

[15]S. Bjørnholm and W. J. Swiatecki, Nucl. Phys. **391**, 471 (1982).

[16]B. Borderie, M. Berlanger, D. Gardes, F. Hanappe, L. Nowicki, J. Peter, B. Tamain, S. Agarwall, J. Girard, C. Gregiore, J. Matuszek, and C. Ngo, Z. Phys. A **288**, 391 (1978).

[17]H. Esbensen, Nucl. Phys. **A352**, 147 (1981).

[18]I. Halpern and V. M. Strutinsky, in *Proceedings of the Second United Nations International Conference on the Peaceful Uses of Atomic Energy* (United Nations, Geneva, Switzerland, 1958), p. 408.

[19]S. Cohen, F. Plasil, and W. J. Swiatecki, Ann. Phys. (N.Y.) **82**, 557 (1974).

[20]Aage Bohr, in *Proceedings of the United Nations International Conference on the Peaceful Uses of Atomic Energy, Geneva, Switzerland, 1955* (United Nations, New York, 1956), Vol. 2, p. 151.

[21]J. Randrup and T. Døssing, Nucl. Phys. **A433**, 215 (1985).

[22]V. E. Viola, Jr., Nucl. Data. **A1**, 391 (1966).

[23]R. Vandenbosch, in *Nuclear Physics with Heavy Ions: Prospects at Energies Below 200 MeV/amu, Nuclear Science Research Conference Series* (Harwood, New York, 1984), Vol. 6, p. 447.

[24]V. E. Viola, Jr. and T. Sikkeland, Phys. Rev. **128**, 767 (1962).

[25]A. Gavron, J. Boissevain, H. C. Britt, K. Eskola, P. Eskola, M. M. Fowler, H. Ohm, J. B. Wilhelmy, T. C. Awes, R. L. Ferguson, F. E. Obershain, F. Plasil, and G. L. Young, submitted to Phys. Rev. C.

[26]C.-C. Sahm, H.-G. Clerc, K.-H. Schmidt, W. Reisdorf, P. Armbruster, F. P. Hessberger, J. G. Keller, G. Münzenberg, and D. Vermeulen, Z. Phys. **319**, 113 (1984).